Thalamic stimulation induced changes in network connectivity and excitability in epilepsy

Nicholas M. Gregg,[1] Gabriela Ojeda Valencia,[2] Tereza Pridalova,[1] Harvey Huang,[3] Vaclav Kremen,[1, 4] Brian N. Lundstrom,[1] Jamie J. Van Gompel,[5] Kai J. Miller,[5] Gregory A. Worrell,[1†] Dora Hermes[2†]

Abstract

Background: The clinical effects of deep brain stimulation for neurological conditions manifest across multiple timescales, spanning seconds to months, and involve direct electrical modulation, neuroplasticity, and network reorganization. In epilepsy, the delayed effects of deep brain stimulation on seizures limit optimization. Single pulse electrical stimulation and the resulting pulse evoked potentials offer a measure network effective connectivity and excitability. This study leverages single pulse and high frequency thalamic stimulation during stereotactic electroencephalography to assess seizure network engagement, modulate network activity, and track changes in excitability and epileptiform abnormalities.

Methods: Ten individuals with drug resistant epilepsy undergoing clinical stereotactic electroencephalography were enrolled in this retrospective cohort study. Each underwent a trial of high frequency (145 Hz) thalamic stimulation. Pulse evoked potentials were acquired before and after high frequency stimulation. Baseline evoked potential root-mean-square amplitude assessed seizure network engagement, and modulation of amplitude (post high frequency stimulation versus baseline; Cohen's *d* effect size) assessed change in network excitability. Interictal epileptiform discharge rates were measured by an automated classifier at baseline and during high frequency stimulation. Statistical significance was determined using paired-sample t-tests ($p<0.05$ significance level). This study was approved by the Mayo Clinic Institutional Review Board, with informed consent obtained from all participants.

Results: Thalamic stimulation delivered for >1.5 hours significantly reduced pulse evoked potential amplitudes in connected areas compared to baseline, with the degree of modulation correlated with baseline connectivity strength. Shorter stimulation durations did not induce

reliable changes. High frequency stimulation immediately suppressed interictal epileptiform discharge rates in seizure networks with strong baseline thalamocortical connectivity. Pulse evoked potentials delineated the anatomical distribution of network engagement, revealing distinct patterns across thalamic subfields.

Conclusion: Pulse evoked potentials and thalamic stimulation during stereotactic electroencephalography provide novel network biomarkers to evaluate target engagement and modulation of large-scale networks across acute and subacute timescales. This approach demonstrates potential for efficient, data-driven neuromodulation optimization, and a new paradigm for personalized deep brain stimulation in epilepsy.

Author affiliations:

1. Department of Neurology, Mayo Clinic, Rochester, MN, 55905, USA
2. Department of Physiology and Biomedical Engineering, Mayo Clinic, Rochester MN, 55905, USA
3. Medical Scientist Training Program, Mayo Clinic, Rochester MN, 55905, USA
4. Czech Institute of Informatics, Robotics, and Cybernetics, Czech Technical University in Prague, Prague, 160 00, Czech Republic
5. Department of Neurosurgery, Mayo Clinic, Rochester, MN, 55905, USA

[†] contributed equally

Correspondence to: Nicholas Gregg, MD

200 First Street South Wester, Rochester, MN, 55905.

gregg.nicholas@mayo.edu

Dora Hermes, PhD: hermes.dora@mayo.edu

Gregory Worrell, MD PhD: worrell.gregory@mayo.edu

Running title: Thalamic stimulation in epilepsy

Key words: deep brain stimulation; neuromodulation; effective connectivity; electrophysiology; epilepsy.

Introduction

Deep brain stimulation (DBS) is a viable treatment for a variety of drug-resistant neurological conditions. However, the mechanisms by which DBS modulates large-scale brain networks remain unresolved. Clinical effects of DBS manifest over different timescales, with variability in response rates and symptom improvement across disorders. Particularly favorable outcomes are observed in disorders with well-defined pathological circuits and when DBS effects on clinical symptoms are immediate, allowing for rapid screening and parameter optimization (e.g. Parkinson's disease, essential tremor)[1].

In contrast, conditions such as epilepsy[2], central pain[3], dystonia[4,5], and neuropsychiatric conditions[6,7], the DBS related effects require neuroplasticity or reorganization, which can take hours to months to observe[8], with generally less favorable outcomes when compared to tremor disorders. Epilepsy, a brain network disorder[9-11], is notable for cross-subject heterogeneity with subject-specific seizure network (SN) structures[12]. Furthermore, the primary clinical manifestation of epilepsy[13]—epileptic seizures—have highly dynamic risk profiles[14] with inter-seizure intervals ranging from hours to months. These features present challenges for targeting DBS electrodes to engage and individual's SN and tuning stimulation parameters across a massive potential stimulation parameter space.

In this study, we present an electrophysiological biomarker that rapidly quantifies network-level changes in connectivity and excitability, with the goal of guiding therapeutic neuromodulation for epilepsy. During stereotactic electroencephalography (sEEG) for individuals with drug resistant focal epilepsy, a number of multi-contact penetrating depth electrodes are used to map and characterize pathological networks and identify eloquent structures. Single pulse electrical stimulation can evoke characteristic responses in connected regions, termed pulse evoked potentials (PEPs), which map effective connectivity throughout the network[15,16]. Effective connectivity reflects the causal influence of a stimulated site on other brain regions, and analysis of PEPs over time can be used to quantify changes in network excitability[17-19].

Interictal epileptiform discharges (IEDs), a hallmark subclinical electrophysiological feature of epilepsy[13], are brief paroxysmal bursts of hypersynchronous neuronal firing, detectable via EEG. In this study, we test whether PEPs—acting as biomarkers of network effective

connectivity and excitability—can quantify meaningful neural changes induced by high frequency (HF) thalamic DBS, a proven therapy for reducing seizures in drug resistant epilepsy[2]. We also assess the ability of PEPs to predict DBS modulation of SN IEDs.

Materials and Methods

This research is a retrospective series evaluating the effects of clinical HF-DBS delivered during sEEG monitoring for drug resistant focal epilepsy. Electrical stimulation for mapping thalamocortical networks before and after HF-DBS was performed under Mayo Clinic Institutional Review Board approved protocol (IRB #15-006530). Patients were enrolled at the Mayo Clinic between June 2020 and December 2022. All patients in the study completed a written informed consent. Thalamic leads were placed per clinical care and were not influenced by this study. The thalamic lead targets were selected by the clinical surgical epilepsy conference consensus recommendations. Thalamic targets were patient specific and guided by the hypothesized SN. Clinical stimulation trials are completed to assess stimulation effects on the SN and tolerability, with the advantage of high-quality local field potential recordings from distributed brain regions (up to 256 recording contacts, Natus Quantum amplifier).

Patient characteristics are listed in Table 1. There was some heterogeneity in the clinical HF-DBS parameters. Patient 1 completed bilateral anterior thalamus HF-DBS trial stimulation. Patient 6 underwent single pulse stimulation at baseline, after 1 hour of HF-DBS, and again after 5.8 hours of HF-DBS (listed HF-DBS durations reflect only the active phase of duty-cycle stimulation, e.g. Patient 4 with a 1 min. on 3 min. off duty-cycle received 4.3 hr. of active stimulation, interleaved with 12.9 hr. of off-phase time).

Single pulse electrical stimulation occurred in the awake state prior to and following (within 1-hour) HF-DBS. Bipolar single pulse stimulation was delivered through neighboring contacts on the same lead, using symmetric charge balanced biphasic stimulation pulses with leading cathodal phase, delivered at 0.2 Hz, for 10-15 repetitions. Single pulse stimulation was delivered by a Natus Nicolet stimulator (Patients 1, 2, 7, 9), g.tec g.ESTIM PRO with g.HiAmp amplifier (Patients 4, 8), or Medtronic external neurostimulator 37022 (Patients 3, 5, 6, 10). Current clamped systems (Natus and g.tec) stimuli used amplitudes of 4-6 mA, and voltage clamped (Medtronic) systems used 6-8 V (typical impedance 1-2.5 kilohms; consistent voltage

used at baseline and post-DBS). The g.tec stimulator used pulse widths of 100 microseconds, while the two other systems used 200 microseconds. The Medtronic external neurostimulator was used to deliver HF (145 Hz) thalamic stimulation for all subjects.

Thalamocortical evoked potential data were first cleaned of stimuli with excessive artifact. High pass (1 Hz), low pass (170 Hz) and bandstop (for 60 Hz line noise and harmonics (120 Hz and 180 Hz)) filtering was performed with fourth order Butterworth filters, with forward-reverse filtering to correct for phase distortion. Voltage trace baseline correction consisted of subtracting the median value for window 200 to 50 milliseconds pre-stimulus from the tracing. Lastly, adjusted common average referencing was performed as previously described[20].

To quantify the strength of effective connectivity, baseline PEP root-mean-square (RMS) amplitude was calculated over time window 20 milliseconds through 300 milliseconds post single pulse stimulus. The statistical significance of evoked potentials was assessed by paired-sample t-test, comparing RMS amplitude over this window to a pre-stimulation period of equal duration (480 to 200 milliseconds pre-stimulus, which avoids the baseline correction window). Changes in network excitability are thought to modulate the amplitude of stimulation evoked measures of effective connectivity. Here, modulation of excitability by HF stimulation was evaluated using Cohen's *d*, as has been used previously[17], with Cohen's *d* effect size equal to the difference in mean evoked potential RMS amplitude (post-HF DBS vs. baseline) divided by the pooled standard deviation. A linear regression model, using Ordinary Least Squares evaluated the association between baseline effective connectivity, and HF stimulation induced changes in network excitability. The impact of short versus long durations of HF-DBS on effective connectivity was assessed by comparing the slopes of the linear regression model between the two categories, using the two-sample t-test.

SN IEDs were quantified using a validated classifier[21,22]. The SN was defined by the clinical record and iEEG review. IEDs were assessed in the awake state to avoid confounding by well-known wake/sleep-state dependent changes in IED rates. Behavioral state was determined as previously described[23]. The average spike rate of SN contacts, in the awake state, was assessed over 1 to 12 hours at baseline and 2-15 hours with active DBS. Of note, patient 7 completed a trial of rapid-cycling HF-DBS (2 hours 7 minutes), with duty-cycle of 10 sec. on 10 sec. off, and IED rate data was drawn from this trial. This was used due to the observation by the

clinical team that this patient had return of IEDs following a brief period of suppression at the 1 min. active-phase onset for each typical duty-cycle completed earlier. (Rapid cycling stimulation trial occurred after the post HF-DBS PEPs were measured, and PEP results were from the conventional duty-cycle regime (Table 1)).

Post-operative CT, and pre-operative T1-weighted MRI (MPRAGE) images were used for lead localization. Open source Lead DBS imaging package (v2.5.3) was used for thalamus electrode localization relative to the Krauth/Morel atlas[24], adjusted for use with the Montreal Neurological Institute (MNI) 2009b asymmetric template space used in the Lead-DBS package. Extra-thalamic lead localization and patient specific image rendering was performed using FreeSurfer 7 and custom scripts (available at Multimodal Neuroimaging Lab (MNL) GitHub: https://github.com/MultimodalNeuroimagingLab), along with the Destrieux atlas[25]. Group electrode renderings in Montreal Neurological Institute (MNI) space were completed using SPM12 and custom scripts (MNL GitHub). Analysis of interictal epileptiform discharges was performed using Python (v3.10.13, Python Software Foundation); all other analyses were performed using MATLAB (v2020b, MathWorks). Data and code to reproduce the main findings of this study are available on GitHub (https://github.com/nmgregg/Thalamic-stim-connect).

Results

Eleven subjects with drug resistant epilepsy underwent clinical sEEG monitoring including a thalamic lead, completed a trial of thalamic HF-DBS delivered through sEEG electrodes, and had PEPs collected prior to and following HF-DBS. One subject was excluded due to high impedance thalamic contacts and poor energy delivery during stimulation. Patient characteristics, sEEG lead location, and treatment stimulation parameters were selected based on the clinical evaluation (Table 1). To quantify modulation of thalamocortical effective connectivity (thalamocortical PEPs), single pulses of electrical stimulation were delivered to the thalamus at baseline and following HF-DBS (Figure 1C). Pulse evoked potential RMS amplitude was calculated over the interval 20-300 milliseconds post single pulse stimulus for each recording contact. The time window was chosen to encompass typical N1 and N2 latencies while omitting potential stimulation artifact[15]. The baseline and post HF-DBS PEP amplitudes are shown in Fig.

1D for patient 3, illustrating a reduction in evoked response amplitude after a period of HF-DBS. The change in PEP amplitude has been argued to indicate changes in network excitability[17].

Thalamocortical effective connectivity was assessed in 10 patients, with a total of 11 thalamus leads (Figure 2A). Per clinical decision, thalamus electrodes primarily targeted the anterior thalamus (n=9 subjects), with active contacts in the anterior complex (anteromedial (AM) and anteroventral (AV) nuclei) or ventral group (ventral anterior (VA) and ventrolateral (VL) nuclei). One patient had electrodes in the medial pulvinar (PulM). To define the 11 thalamic electrodes locations we mapped the contacts onto MNI template space, overlayed on the Krauth/Morel thalamus atlas[24], using the Lead-DBS imaging package (v2.5.3)[26], and the BigBrain 3D human brain model[27] (Figure 2).

Thalamocortical effective connectivity is suppressed after >1.5 hours of high frequency DBS

Patients underwent HF-DBS for varying durations, and the active phase of duty-cycle HF-DBS was computed for each. For example, patient 4, with a 1-minute on / 3-minute off duty-cycle received 4.3 hours of active HF-DBS with 12.9 hours of off-phase time. Representative evoked potentials at baseline and post HF-DBS are shown for two subjects (Fig. 2B). For patient 2, who received less than 1.5 hours of stimulation, the evoked potential amplitude remained similar between baseline and post HF-DBS. However, for patient 3, who received >1.5 hours of HF-DBS, there was a clear reduction in evoked potential amplitude.

At the group level, the effect size of HF-DBS modulation of thalamocortical effective connectivity was calculated using Cohen's *d*, comparing the amplitude of PEPs in the post HF-DBS period to the baseline recording that preceded HF-DBS. Figure 2C shows a clear separation in induced changes in PEP amplitude based on the HF-DBS duration. Stimulation lasting more than 1.5 hours consistently resulted in suppression of PEP amplitude (negative Cohen's *d*), while shorter durations showed no effect (zero or positive Cohen's d). Furthermore, the effects of modulation were greatest for areas with strong baseline connectivity (Fig. 2C).

A linear regression model comparing baseline PEP amplitudes and the degree of HF-DBS induced modulation revealed different responses between short- and long-duration HF-DBS groups (P = 0.0016; 95% confidence interval of the difference in mean slope = [-1.53, -0.48]).

Thus, baseline effective connectivity predicted the effect size of PEP suppression following >1.5 hours of HF-DBS. Patient-specific regression model metrics are in Supplemental Table 2.

The effects of thalamic high frequency DBS are network specific

The anatomical distribution of stimulation-induced changes is shown in glass brain renderings (Fig. 3). HF-DBS of distinct thalamic subfields affected different networks, with patterns varying across anteromedial nucleus (patient 1 right and left, and patient 3), ventral anterior nucleus (patients 2, 6, and 8), ventrolateral nucleus (patients 5 and 9), and medial pulvinar (patient 4). Supplemental Figure 1 shows electrode position and relevant thalamic nuclei. Single pulse stimulation of the anteromedial nucleus at the junction with anteroventral and ventral anterior nuclei resulted in more widespread projections than other subfields, with statistically significant PEPs observed in 95% (±0.6%) of recording contacts for anteromedial stimulation, compared to 37% (±26%) for non-anteromedial nucleus stimulation (median (standard deviation)). Single pulse stimulation of the anteromedial, ventral anterior, ventrolateral, and medial pulvinar nuclei had preferential engagement of frontotemporal limbic, prefrontal, motor/premotor, and posterior quadrant patterns of connectivity, respectively. Figure 3 also demonstrates the HF-DBS duration-dependent changes in effective connectivity: in patient 6 in particular the stronger network modulation after 5.8 hours of HF-DBS can be compared to weak effects after 1 hour of HF-DBS, with selected PEP tracings shown in Supplemental Figure 2.

Thalamic high frequency DBS modulates interictal epileptiform discharges in a network-selective manner

Figures 2-3 show that thalamocortical PEPs were modulated by HF-DBS in a manner that was highly network specific and influenced by baseline PEP strength. To directly assess the relevance of these findings for epilepsy, we assessed the impact of HF-DBS on IEDs—a well-established biomarker of epilepsy network activity—and characterized the association between baseline thalamocortical effective connectivity and IED rate modulation. Using a validated IED classifier[21], we compared the rate of IEDs during awake baseline (immediately preceding the stimulation trial) and DBS phases. Interestingly, the effect of HF-DBS on IEDs was immediate

and was observable between the on- and off-phases of duty-cycle stimulation for some individuals (Fig. 4A), in contrast to the delayed modulation of PEP amplitude.

We propose three models to describe the relationship between baseline thalamocortical connectivity and IED rate modulation: 1) IED modulation is independent of the baseline connectivity (Fig. 4B); 2) IED modulation depends on electrode-specific baseline connectivity (Fig. 4C); or 3) IED modulation depends on average subject specific SN connectivity, reflecting overall network engagement (Fig. 4D). The data best fit the third model, where greater explained variance and group separation were observed based on average SN connectivity (Fig. 4). These findings align with the concept that epilepsy is a network disease[9-12], with IED modulation dependent on the extent to which HF-DBS engages the entire SN.

Discussion

Rapid electrophysiological biomarkers are needed to assess network engagement and track excitability for neuromodulation of disorders with diverse networks and delayed clinical effects, such as focal epilepsy. Our findings identify such a biomarker of DBS in a cohort of individuals with drug-resistant epilepsy undergoing stereotactic EEG. Across the cohort, thalamocortical evoked potential amplitude was significantly reduced in a network selective manner after >1.5 hours of thalamic HF-DBS. Importantly, these effects were specific to the engaged anatomical network, as indicated by baseline PEPs, and IED suppression was only observed when thalamic stimulation sufficiently engaged the seizure network. These results demonstrate that thalamocortical effective connectivity, assessed by single-pulse electrical stimulation, can capture network engagement and DBS-induced changes in network excitability.

This work offers several key insights into the effects of thalamic DBS. First, changes in effective connectivity depend on the duration of stimulation, with consistent suppression of network excitability—measured by change in effective connectivity—occurring after >1.5 hours of active HF-DBS (>780,000 pulses). Second, thalamic HF-DBS induced excitability changes depend on the baseline strength of thalamocortical connections, which can be mapped using PEPs to characterize the anatomical distribution and strength of connectivity. Third, HF-DBS acutely modulates pathological interictal SN activity, as reflected by changes in the rate of IEDs,

and depends on overall SN engagement. This timescale is consistent with direct electrical effects of stimulation.

The electrophysiological biomarkers characterized in this work could be applied to personalize neuromodulation. The development of adaptive, sensing-capable DBS systems (ClinicalTrials.gov ID NCT04547712, “Adaptive DBS Algorithm for Personalized Therapy in Parkinson's Disease”) underscores the importance of identifying electrophysiological biomarkers to guide the next generation of neuromodulation. Evoked response measures of effective connectivity and the tracking of IEDs can demonstrate network engagement, assess subacute changes in network excitability (e.g. plasticity), and quantify the acute electrical modulation of pathological SN activity (IEDs). Importantly, previous work with transcranial magnetic stimulation[28] and responsive neurostimulation[29] has shown that stimulation-evoked measures of excitability and IED rate are correlated with long-term seizure control. These biomarkers may aid in precise electrode targeting to optimize SN engagement, and enable efficient, data-driven tuning of stimulation parameters.

The relatively long duration of HF-DBS required to induce changes in thalamocortical effective connectivity suggests neuroplasticity-based changes in neuronal activity, such as homeostatic plasticity[30,31]. Homeostatic plasticity mechanisms, such as synaptic scaling[32] and regulation of intrinsic excitability[33], stabilize network activity and neuron firing rates when exposed to a perturbation that disrupts the existing equilibrium. These mechanisms operate over hours-long timescales, consistent with the timescale of DBS-induced modulation observed here, and parallel the clinical effects of DBS seen in disorders such as Tourette syndrome (motor tics), Parkinson’s disease (bradykinesia), central pain, and mood disorders[8]. Thus, HF-DBS may trigger a homeostatic response that reduces SN excitability which can ultimately lower the seizure burden.

Whereas HF-DBS elicited changes in network excitability measured with evoked responses only after about 1.5 hours of active stimulation, HF-DBS acutely suppressed SN IED rate. These two electrophysiological biomarkers characterize different aspects of network modulation. The acute effects of HF-DBS on IED modulation, as seen here, have been linked to the desynchronization of local field activity[34]. Similarly, immediate tremor improvements seen with DBS for essential tremor and Parkinson’s disease, are attributed in part to an “informational lesion” or “jamming” of pathological low-frequency oscillatory circuit activity[35,36].

The SN IED rate modulation depended on overall SN engagement, as measured by baseline thalamocortical PEP amplitude across all SN contacts (Fig. 4). This aligns with a network model of epilepsy[9] in which sufficient engagement of network nodes modulates the broader pathological network[10], including subregions with poor thalamocortical connectivity. Additionally, these results provide unique electrophysiological evidence supporting a previously proposed "network theory" of ANT-DBS[37], and are consistent with the connectivity dependence of clinical outcomes with DBS for other neurological disorders[38-41]. Biomarkers to track changes in network activity (PEP-based neuroplastic changes, IED-based direct electrical modulation) may provide distinct and complementary insights into the effects of stimulation to guide parameter optimization. This work should motivate further research into network-guided neuromodulation for epilepsy[12], and biomarkers of network engagement and modulation could have applications beyond epilepsy.

This study also provides strong evidence that the anatomical distribution of DBS effects differs between neighboring subfields of the anterior thalamus and pulvinar (Fig. 3). It is important to note that these stimulation derived connectivity maps provide information that is distinct from and complementary to thalamic seizure recordings[42,43]—this is a critical distinction with underappreciated relevance to patient care due to inconsistent reciprocity in cortico-thalamic and thalamo-cortical connectivity[44] (the thalamic nucleus with maximal ictal activity is not necessarily the thalamic DBS target that will best engage the seizure network). The largest spread of DBS effects was observed when stimulation fields engaged the anteromedial nucleus (AM) at the junction with the anteroventral (AV) and ventral anterior (VA) nuclei (AM and AV comprising two of the three ANT nuclei). This finding may clarify and provide a mechanistic rationale for electrode targeting for ANT-DBS, an unresolved issue[45-47]. We propose that targeting the AM/AV/VA junction provides broader engagement of limbic and prefrontal systems, whereas the AV nucleus—a common target in epilepsy DBS surgery—has more restricted projections to the anterior limbic system[48] (orbitofrontal, cingulate, medial prefrontal cortex). Ultimately, DBS target selection that maximizes engagement of an individual's SN may outperform a generic target.

This study is limited by the relative rarity of human thalamic sEEG and the complexity of clinical care in the epilepsy monitoring unit. The HF-DBS trials were delivered as a part of clinical care, contributing to variability in thalamic targets, stimulation parameters, and HF-DBS

duration. One patient had resumption of antiseizure medications between the baseline and post-DBS PEP measurements, which may have impacted brain excitability. More research is needed to assess for differential effects of DBS across thalamic nuclei, and evaluate thalamic subfield effective connectivity with respect to functional connectivity[49]. Further research is needed to evaluate how the HF-DBS effects reported here may inform chronically implanted and adaptive DBS systems[50].

This work leverages multi-contact sEEG, including thalamic coverage, and employs single-pulse and repetitive thalamic stimulation to provide important insights into the effects of thalamic stimulation on brain networks across multiple timescales. Our findings demonstrate the critical importance of SN engagement for DBS efficacy. To improve epilepsy neuromodulation, individualized, data-driven approaches are needed. This study characterizes electrophysiological biomarkers—using straightforward methods—that may enable a new model of biomarker targeted stimulation, facilitating data-driven tuning of stimulation parameters[51], and individualized targeting to optimize network engagement. These tools may advance a highly personalized approach to DBS to improve patient care.

Data availability

Data and code to reproduce the main findings of this study are available by reasonable request.

Funding

National Institute of Neurological Disorders and Stroke awards K23NS136792, R01NS09288203, and National Institute of Mental Health award R01MH122258.The content is solely the responsibility of the authors and does not represent the official views of the NIH. The CLARA project that has received funding from the European Union’s HORIZON EUROPE research and innovation program, Grant Agreement No 101136607.

Competing interests

N.M.G. is an industry consultant (NeuroOne, funds to Mayo Clinic). G.A.W. declares intellectual property has been licensed to Cadence Neuroscience and NeuroOne. G.A.W serves on scientific advisory board for NeuroOne Inc., UNEEG Inc., LivaNova Inc., and NeuroPace Inc. and Cadence Neuroscience Inc. B.N.L. declares intellectual property licensed to Cadence Neuroscience (contractual rights waived) and Seer Medical (contractual rights waived); and has been a site investigator (Medtronic EPAS, NeuroPace RESPONSE, Neuroelectrics tDCS for Epilepsy) and industry consultant (Epiminder, Medtronic, Neuropace, Philips Neuro; funds to Mayo Clinic). J.J.V.G. was named inventor for intellectual property licensed to Cadence Neuroscience, and has been an investigator for the Medtronic EPAS trial, SLATE trial, and Mayo Clinic Medtronic NIH Public Private Partnership (UH3-NS95495); has owned stock in and has had a consulting contract with Neuro-One; and has been site Primary Investigator in the Polyganics ENCASE II trial, site Primary Investigator in the NXDC Gleolan Men301 trial, and site Primary Investigator in the Insightec MRgUS EP001 trial. Remaining authors declare no competing financial interests.

Author Contributions

N.M.G., D.H., G.A.W designed research; N.M.G., D.H., G.A.W., G.O.V, H.H., performed research; N.M.G., D.H., H.H., K.J.M. contributed analytic tools; N.M.G. and D.H. wrote the paper; all authors provided meaningful drafting and editing of the paper.

Supplementary material

Supplementary material is available at Brain online.

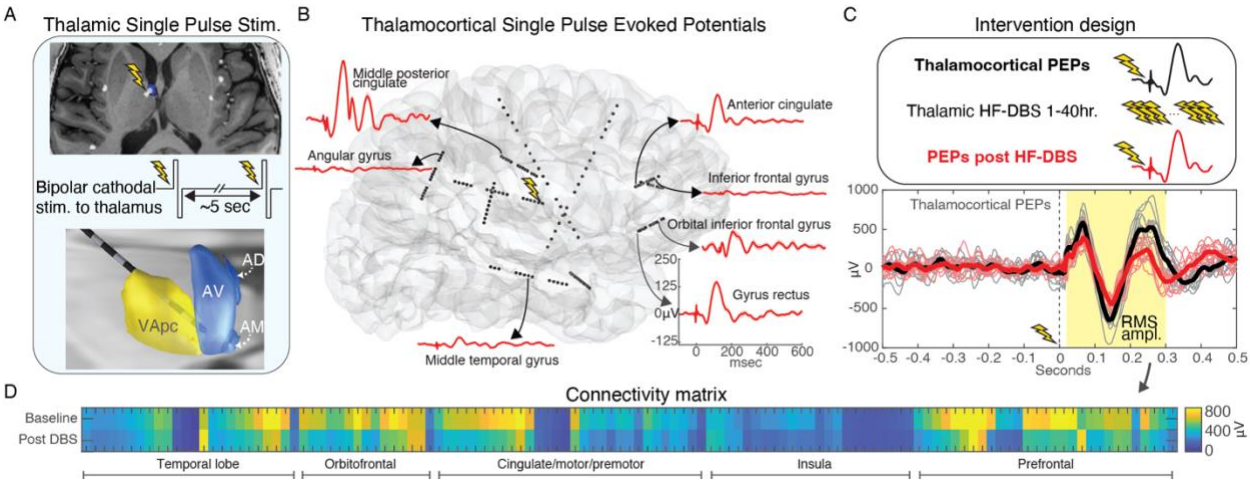

Figure 1. Thalamic high frequency deep brain stimulation and network effective connectivity. A) Bipolar single pulses of electrical stimulation (charge balanced symmetric square wave, leading cathodal phase) are delivered to neighboring thalamic electrode contacts. B) Single pulses delivered to the thalamus produce characteristic evoked responses in connected brain regions, evident in sEEG electrode voltage traces (figure shows representative evoked responses; average trace from n=10 single pulse stimuli). C) Thalamocortical evoked potentials were measured at baseline and following HF-DBS. Single trial and average voltage traces are shown for baseline (black) and post-high frequency stimulation (red). The root-mean-square (RMS) amplitude was calculated over a window [20, 300] ms after the single pulse stimulus, for each recording contact. D) Thalamocortical effective connectivity matrix shows evoked potential RMS amplitude at baseline, and post HF-DBS stimulation, across all contacts, with clear suppression of thalamocortical evoked response amplitude (excitability) over multiple regions. Data from patient 3. AD = anterodorsal nucleus. AV = anteroventral nucleus. AM = anteromedial nucleus. VApc = ventral anterior nucleus, parvocellular division. PEP = pulse evoked potential. HF-DBS = high frequency deep brain stimulation.

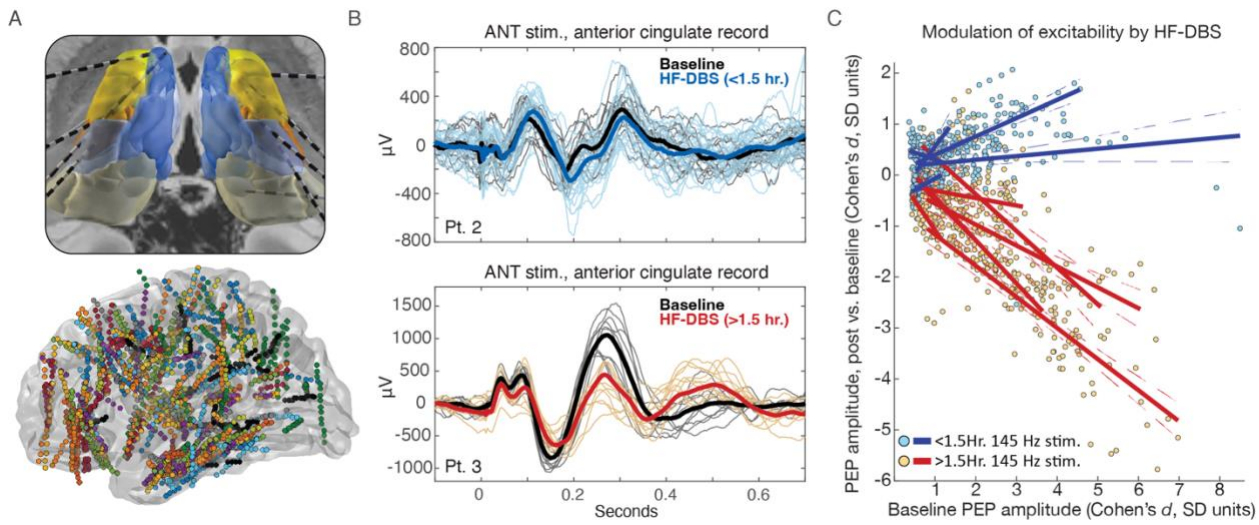

Figure 2. Thalamic high frequency stimulation modulates network effective connectivity and is dependent on baseline connectivity strength, and duration. A) Ten patient cohort with thalamus electrodes (top panel, Krauth/Morel thalamus atlas[24]) and all recording electrodes (bottom panel) shown in MNI template space (right hemisphere electrodes mirrored into left hemisphere). B) Example single trial and average thalamocortical evoked potential (EP) traces from two subjects completing short duration (top panel) and long duration (bottom panel) thalamic HF-DBS. C) Modulation of evoked potential amplitude is dependent on high frequency stimulation duration(>1.5 vs. <1.5 hours of active high frequency stimulation), and the strength of baseline connectivity. Solid lines correspond to linear model fit (dashed lines mark the 95% confidence intervals) for each individual (Patient 1 had bilateral thalamic stimulation and left and right hemispheres treated independently). Plot shows recording electrodes with statistically significant baseline evoked potentials (paired T-test comparing amplitude [20, 300] ms post-single pulse stimulus to [-480, -200] ms pre-single pulse stimulus. Voltage traces undergo baseline correction by subtracting the median value for window [-200, -50] ms pre stimulus, and so this baseline period was omitted)). PEP=single pulse evoked potentials. HF-DBS = high frequency deep brain stimulation.

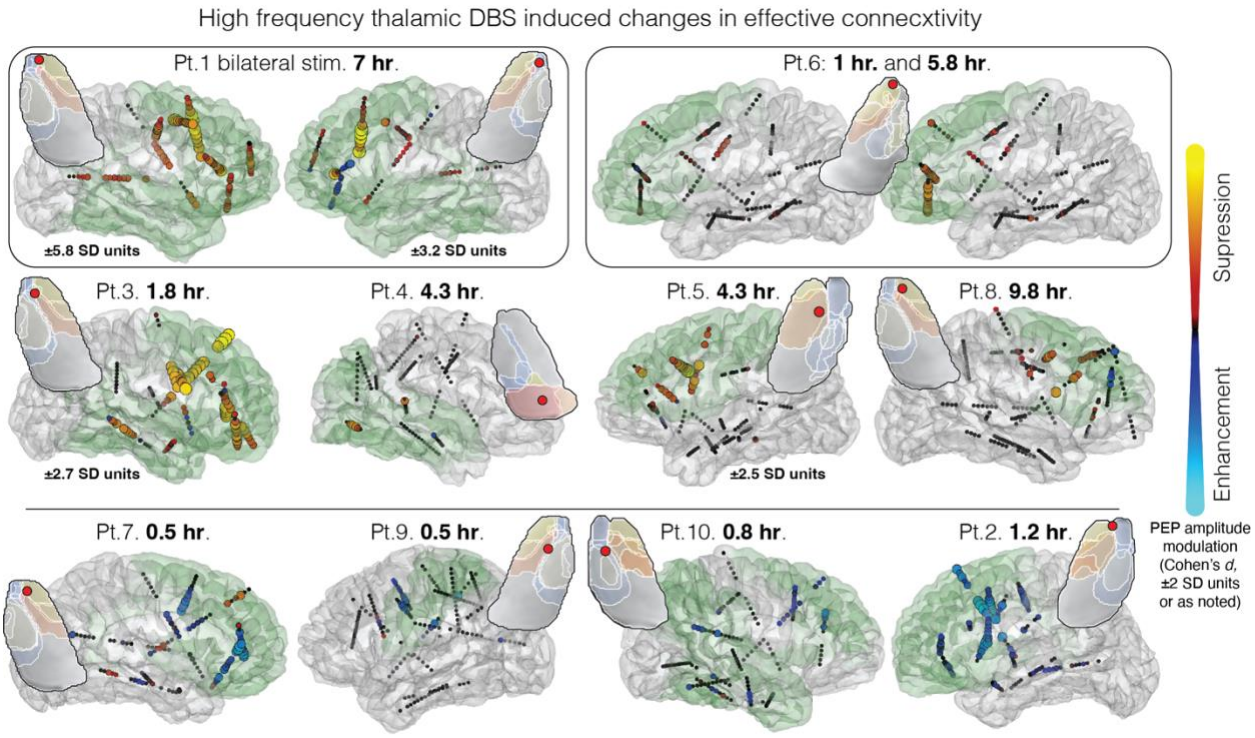

Figure 3. High frequency thalamic stimulation modulates brain excitability, with network specificity and stimulation duration dependence. Brain renderings show thalamic HF-DBS induced changes in network effective connectivity (comparison of baseline and post HF-DBS single pulse evoked potential amplitude, Cohen's *d* effect size, for contacts with statistically significant baseline evoked potentials). Distinct anatomic distributions of effects can be seen between patients—note broad frontotemporal engagement with anteromedial nucleus stimulation (Pt. 1 right and left, and Pt. 3), occipital engagement with medial pulvinar stimulation (Pt. 4), peri-rolandic engagement with ventrolateral nucleus stimulation (Pt. 5 and 9), and prefrontal projections with ventral anterior nucleus stimulation (Pts. 2, 6 and 8). Consistent suppression of effective connectivity is seen with HF-DBS duration >1.5 hours (top and middle row) vs. <1.5 hours (bottom row) (listed HF-DBS duration is the total time of the active phase only of duty-cycle stimulation). The insets show axial thalamic slices (anatomical orientation), the stimulated cathodal contact (red circle), and relevant nuclei. Supplemental Figure 1 shows the stimulated electrode and labeled axial and coronal thalamic slices. Green shading illustrates general estimated projection maps based on prior structural/functional imaging-based connectivity studies[48]. PEP = pulse evoked potential. HF-DBS = high frequency deep brain stimulation. SD = standard deviation.

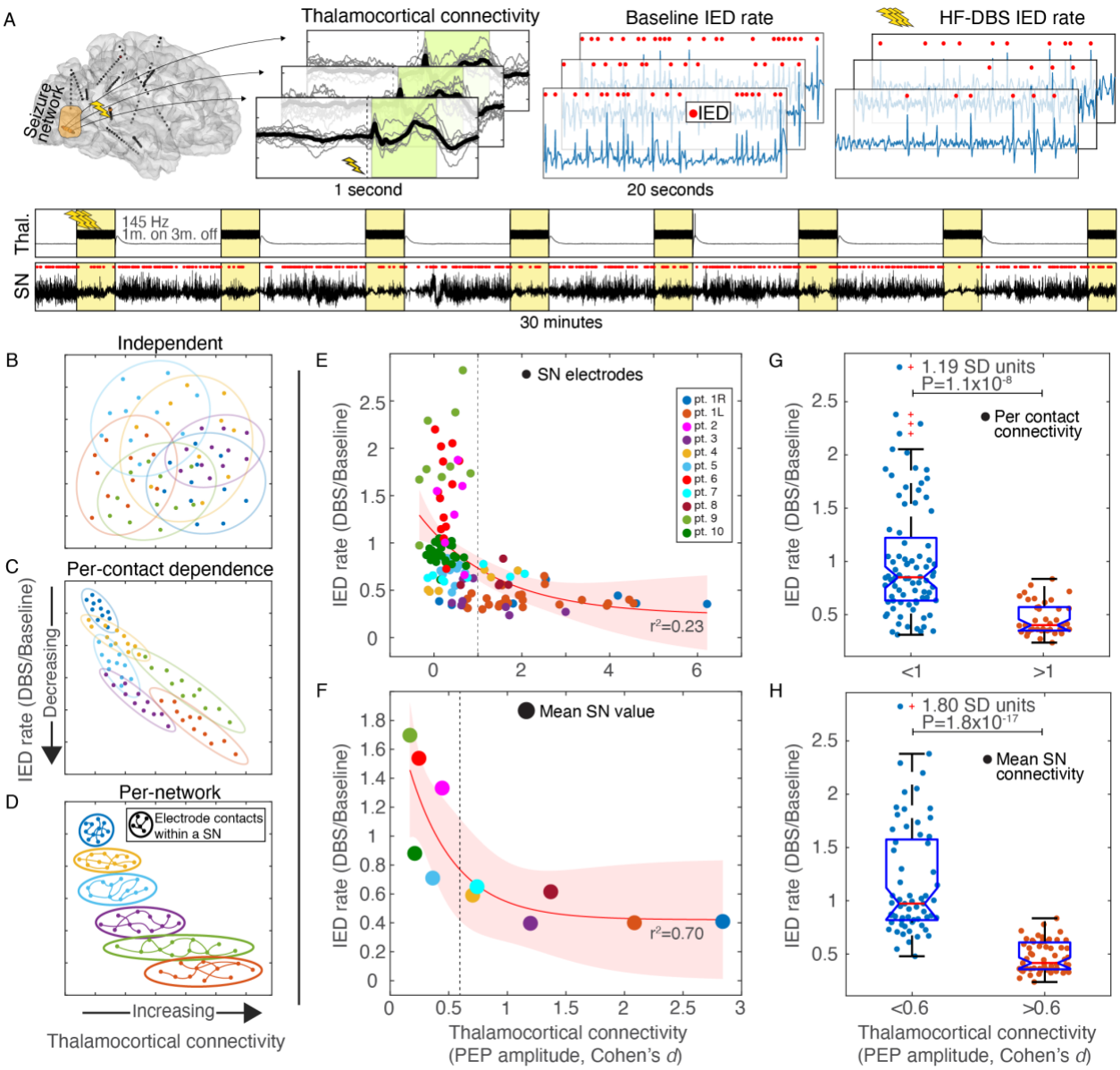

Figure 4. Thalamocortical connectivity predicts the impact of HF-DBS on epileptiform activity (seizure network excitability). A) Baseline PEP amplitude quantified thalamocortical connectivity. IEDs were quantified using a validated classifier in the awake state, at baseline and during HF-DBS; representative data from Pt. 4. Three descriptive models of how thalamocortical connectivity may predict the impact of thalamic HF-DBS on the rate of IEDs: B) baseline connectivity amplitude does not predict DBS modulation of IED rate; C) connectivity amplitude is directly predictive of IED rate modulation, per-contact; D) overall SN engagement (average connectivity amplitude across all SN contacts) is predictive of DBS modulation of IED rate. E) Scatter plot of thalamic HF-DBS induced change in the rate of IED rate, relative to baseline

thalamocortical PEP amplitude, measured from each SN electrode contact; F) corresponding mean SN values. Exponential fit model [$y(x) = a * e^{(-b*x)} + c$] with 95% confidence interval and coefficient of determination are shown in E) and F). G) Box-plot of IED rate modulation per-contact, binarized into low and high per-contact connectivity groups, and H) low and high average SN connectivity groups. *Patient 7 results from rapid-cycling DBS (10 sec. on 10 sec. off). HF-DBS = high frequency deep brain stimulation; SN = seizure network; IED = interictal epileptiform discharge.

Patient	Age	Sex	Seizure onset	Thalamic stim. location	Stimulation parameters	Duration thalamic HF-DBS	Med. change
1	16-20	m	Diffuse bifrontal, left hemisphere lead in	R-AM, AV, VApc; L-AM, AV, VApc	145 Hz, 90 µsec, 5.7mA (total), 1m. on 1m. off	7 hr.	NC
2	46-50	m	Left middle temporal gyrus	L-AV, VApc, VLpd	145 Hz, 90 µs, 3.6mA, continuous	1.2 hr.	NC
3	26-30	m	Bilateral hippocampus, left lead in	R-AM, AV, VApc, VLpv	145 Hz, 200 µs, 3.7mA, 1m. on 1m. off	1.8 hr.	NC
4	11-15	m	Right occipital, peri-lesion (perinatal stroke)	R-PulM	145 Hz, 200 µs, 5.8mA, 1m. on 3m. off	4.3 hr.	change (increase LTG, restart ZNS)
5	16-20	f	Left hippocampus, peri-lesion (neoplasm)	L-VLpd	145 Hz, 200 µs, 4.6mA, 1m. on 3m. off	4.3 hr.	NC
6	66-70	f	Left neocortical and mesial temporal	L-VApc*	145 Hz, 200 µs, 4.3mA, 1m. on 3m. off	1 hr.; 5.8 hr.	NC

7	41-45	m	Bilateral anterior cingulate	R-VApc, AV	145 Hz, 200 µs, 2.5mA, 1m. on 3m. off	0.5 hr.	NC
8	16-20	f	Right neocortical temporal	R-VApc, VLpv*	145 hz, 200 µs, 3.3mA, 1m. on 3m. off	9.8 hr.	NC
9	6-10	f	Pre- and post-central gyri, peri-lesion (FCD)	L-VLpv	145 Hz, 200 µs, 2.8mA, 1m. on 5m. off	0.5 hr.	NC
10	16-20	f	Multifocal, right anterior/middle insula, amygdala, temporal neocortex	R-CL, AV, MDpc	145 Hz, 90 µs, 3.2mA, 1m. on 5m. off	0.8 hr.	Rescue IV lorazepam & LEV pre-baseline

Table 1. Patient characteristics. The duration of thalamic high frequency deep brain stimulation (HF-DBS) is the active stimulation time (does not include off-phase of duty-cycle stimulation). Patient 6 completed single pulse stimulation after 1-hour and 5.8-hours of HF-DBS. L=left. R=right. FCD=focal cortical dysplasia. ANT=anterior nucleus of the thalamus. Thalamic nuclei abbreviations, Krauth/Morel atlas[24]. PulM=medial pulvinar. AM=anteromedial nucleus. AV=anteroventral nucleus. VApc=ventral anterior nucleus, parvocellular division. VLa=ventral lateral anterior nucleus. VLpv=ventral lateral posterior nucleus, ventral division. Duty-cycle (on-period and off-period) noted in minutes. NC=no change in medication regimen during the single-pulse and HF-DBS period. LEV=levetiracetam. LTG=lamotrigine. ZNS=zonisamide.
*Additional cortical stimulation site (Supplemental Table 1).

References

1. Schuepbach WM, Rau J, Knudsen K, et al. Neurostimulation for Parkinson's disease with early motor complications. *N Engl J Med.* 2013;368(7):610-622.
2. Fisher R, Salanova V, Witt T, et al. Electrical stimulation of the anterior nucleus of thalamus for treatment of refractory epilepsy. *Epilepsia.* 2010;51(5):899-908.
3. Boccard SG, Pereira EA, Aziz TZ. Deep brain stimulation for chronic pain. *J Clin Neurosci.* 2015;22(10):1537-1543.
4. Tisch S, Rothwell JC, Bhatia KP, et al. Pallidal stimulation modifies after-effects of paired associative stimulation on motor cortex excitability in primary generalised dystonia. *Exp Neurol.* 2007;206(1):80-85.
5. Krauss JK, Yianni J, Loher TJ, Aziz TZ. Deep brain stimulation for dystonia. *J Clin Neurophysiol.* 2004;21(1):18-30.
6. Alagapan S, Choi KS, Heisig S, et al. Cingulate dynamics track depression recovery with deep brain stimulation. *Nature.* 2023;622(7981):130-138.
7. Crowell AL, Garlow SJ, Riva-Posse P, Mayberg HS. Characterizing the therapeutic response to deep brain stimulation for treatment-resistant depression: a single center long-term perspective. *Front Integr Neurosci.* 2015;9:41.
8. Ashkan K, Rogers P, Bergman H, Ughratdar I. Insights into the mechanisms of deep brain stimulation. *Nat Rev Neurol.* 2017;13(9):548-554.
9. Morgan RJ, Soltesz I. Nonrandom connectivity of the epileptic dentate gyrus predicts a major role for neuronal hubs in seizures. *Proc Natl Acad Sci U S A.* 2008;105(16):6179-6184.
10. Wilke C, Worrell G, He B. Graph analysis of epileptogenic networks in human partial epilepsy. *Epilepsia.* 2011;52(1):84-93.
11. Richardson MP. Large scale brain models of epilepsy: dynamics meets connectomics. *J Neurol Neurosurg Psychiatry.* 2012;83(12):1238-1248.
12. Piper RJ, Richardson RM, Worrell G, et al. Towards network-guided neuromodulation for epilepsy. *Brain.* 2022;145(10):3347-3362.
13. Fisher RS, Acevedo C, Arzimanoglou A, et al. ILAE official report: a practical clinical definition of epilepsy. *Epilepsia.* 2014;55(4):475-482.

14. Karoly PJ, Rao VR, Gregg NM, et al. Cycles in epilepsy. *Nature Reviews Neurology.* 2021.
15. Keller CJ, Honey CJ, Megevand P, Entz L, Ulbert I, Mehta AD. Mapping human brain networks with cortico-cortical evoked potentials. *Philos Trans R Soc Lond B Biol Sci.* 2014;369(1653).
16. van Blooijs D, van den Boom MA, van der Aar JF, et al. Developmental trajectory of transmission speed in the human brain. *Nat Neurosci.* 2023;26(4):537-541.
17. Keller CJ, Huang Y, Herrero JL, et al. Induction and Quantification of Excitability Changes in Human Cortical Networks. *J Neurosci.* 2018;38(23):5384-5398.
18. Valentin A, Alarcon G, Honavar M, et al. Single pulse electrical stimulation for identification of structural abnormalities and prediction of seizure outcome after epilepsy surgery: a prospective study. *Lancet Neurol.* 2005;4(11):718-726.
19. Matsumoto R, Kunieda T, Nair D. Single pulse electrical stimulation to probe functional and pathological connectivity in epilepsy. *Seizure.* 2017;44:27-36.
20. Huang H, Ojeda Valencia G, Gregg NM, et al. CARLA: Adjusted common average referencing for cortico-cortical evoked potential data. *J Neurosci Methods.* 2024;407:110153.
21. Janca R, Jezdik P, Cmejla R, et al. Detection of interictal epileptiform discharges using signal envelope distribution modelling: application to epileptic and non-epileptic intracranial recordings. *Brain Topogr.* 2015;28(1):172-183.
22. Sladky V, Nejedly P, Mivalt F, et al. Distributed brain co-processor for tracking spikes, seizures and behaviour during electrical brain stimulation. *Brain Commun.* 2022;4(3):fcac115.
23. Dell KL, Payne DE, Kremen V, et al. Seizure likelihood varies with day-to-day variations in sleep duration in patients with refractory focal epilepsy: A longitudinal electroencephalography investigation. *EClinicalMedicine.* 2021:100934.
24. Krauth A, Blanc R, Poveda A, Jeanmonod D, Morel A, Szekely G. A mean three-dimensional atlas of the human thalamus: generation from multiple histological data. *Neuroimage.* 2010;49(3):2053-2062.
25. Destrieux C, Fischl B, Dale A, Halgren E. Automatic parcellation of human cortical gyri and sulci using standard anatomical nomenclature. *Neuroimage.* 2010;53(1):1-15.

26. Horn A, Li N, Dembek TA, et al. Lead-DBS v2: Towards a comprehensive pipeline for deep brain stimulation imaging. *Neuroimage.* 2019;184:293-316.
27. Amunts K, Lepage C, Borgeat L, et al. BigBrain: an ultrahigh-resolution 3D human brain model. *Science.* 2013;340(6139):1472-1475.
28. Pawley AD, Chowdhury FA, Tangwiriyasakul C, et al. Cortical excitability correlates with seizure control and epilepsy duration in chronic epilepsy. *Ann Clin Transl Neurol.* 2017;4(2):87-97.
29. Arcot Desai S, Tcheng TK, Morrell MJ. Quantitative electrocorticographic biomarkers of clinical outcomes in mesial temporal lobe epileptic patients treated with the RNS(R) system. *Clin Neurophysiol.* 2019;130(8):1364-1374.
30. Turrigiano GG. The self-tuning neuron: synaptic scaling of excitatory synapses. *Cell.* 2008;135(3):422-435.
31. Chai Z, Ma C, Jin X. Homeostatic activity regulation as a mechanism underlying the effect of brain stimulation. *Bioelectron Med.* 2019;5:16.
32. Turrigiano GG, Nelson SB. Homeostatic plasticity in the developing nervous system. *Nat Rev Neurosci.* 2004;5(2):97-107.
33. Marder E, Goaillard JM. Variability, compensation and homeostasis in neuron and network function. *Nat Rev Neurosci.* 2006;7(7):563-574.
34. Yu T, Wang X, Li Y, et al. High-frequency stimulation of anterior nucleus of thalamus desynchronizes epileptic network in humans. *Brain.* 2018;141(9):2631-2643.
35. Grill WM, Snyder AN, Miocinovic S. Deep brain stimulation creates an informational lesion of the stimulated nucleus. *Neuroreport.* 2004;15(7):1137-1140.
36. Lozano AM, Lipsman N, Bergman H, et al. Deep brain stimulation: current challenges and future directions. *Nat Rev Neurol.* 2019;15(3):148-160.
37. Salanova V, Sperling MR, Gross RE, et al. The SANTE study at 10 years of follow-up: Effectiveness, safety, and sudden unexpected death in epilepsy. *Epilepsia.* 2021;62(6):1306-1317.
38. Horn A, Reich M, Vorwerk J, et al. Connectivity Predicts deep brain stimulation outcome in Parkinson disease. *Ann Neurol.* 2017;82(1):67-78.

39. Johnson KA, Duffley G, Anderson DN, et al. Structural connectivity predicts clinical outcomes of deep brain stimulation for Tourette syndrome. *Brain.* 2020;143(8):2607-2623.
40. Middlebrooks EH, Okromelidze L, Wong JK, et al. Connectivity correlates to predict essential tremor deep brain stimulation outcome: Evidence for a common treatment pathway. *Neuroimage Clin.* 2021;32:102846.
41. Hollunder B, Ostrem JL, Sahin IA, et al. Mapping dysfunctional circuits in the frontal cortex using deep brain stimulation. *Nat Neurosci.* 2024;27(3):573-586.
42. Wu TQ, Kaboodvand N, McGinn RJ, et al. Multisite thalamic recordings to characterize seizure propagation in the human brain. *Brain.* 2023;146(7):2792-2802.
43. Guye M, Regis J, Tamura M, et al. The role of corticothalamic coupling in human temporal lobe epilepsy. *Brain.* 2006;129(Pt 7):1917-1928.
44. Rosenberg DS, Mauguiere F, Catenoix H, Faillenot I, Magnin M. Reciprocal thalamocortical connectivity of the medial pulvinar: a depth stimulation and evoked potential study in human brain. *Cereb Cortex.* 2009;19(6):1462-1473.
45. Gross RE, Fisher RS, Sperling MR, Giftakis JE, Stypulkowski PH. Analysis of Deep Brain Stimulation Lead Targeting in the Stimulation of Anterior Nucleus of the Thalamus for Epilepsy Clinical Trial. *Neurosurgery.* 2021;89(3):406-412.
46. Lehtimaki K, Mottonen T, Jarventausta K, et al. Outcome based definition of the anterior thalamic deep brain stimulation target in refractory epilepsy. *Brain Stimul.* 2016;9(2):268-275.
47. Schaper F, Plantinga BR, Colon AJ, et al. Deep Brain Stimulation in Epilepsy: A Role for Modulation of the Mammillothalamic Tract in Seizure Control? *Neurosurgery.* 2020;87(3):602-610.
48. Jones EG. *The Thalamus.* Second ed. Cambridge: Cambridge University Press; 2007.
49. Wu D, Schaper F, Jin G, et al. Human anterior thalamic stimulation evoked cortical potentials align with intrinsic functional connectivity. *Neuroimage.* 2023;277:120243.
50. Oehrn CR, Cernera S, Hammer LH, et al. Chronic adaptive deep brain stimulation versus conventional stimulation in Parkinson's disease: a blinded randomized feasibility trial. *Nat Med.* 2024.

51. Stieve BJ, Richner TJ, Krook-Magnuson C, Netoff TI, Krook-Magnuson E. Optimization of closed-loop electrical stimulation enables robust cerebellar-directed seizure control. *Brain.* 2023;146(1):91-108.